Talanta 84 (2011) 89–97

Contents lists available at ScienceDirect

Talanta

journal homepage: www.elsevier.com/locate/talanta

Preparation of anti-CD4 monoclonal antibody-conjugated magnetic poly(glycidyl methacrylate) particles and their application on CD4$^+$ lymphocyte separation

Nuttaporn Pimpha[a,*], Saowaluk Chaleawlert-umpon[a], Nuttapol Chruewkamlow[b], Watchara Kasinrerk[b,c,**]

[a] National Nanotechnology Center, National Science and Technology Development Agency, 113 Thailand Science Park, Paholyothin Rd., Pathumthani 12120, Thailand
[b] Biomedical Technology Research Center, National Center for Genetic Engineering and Biotechnology, National Sciences and Technology Development Agency at the Faculty of Associated Medical Sciences, Chiang Mai University, Chiang Mai 50200, Thailand
[c] Division of Clinical Immunology, Department of Medical Technology, Faculty of Associated Medical Sciences, Chiang Mai University, Chiang Mai 50200, Thailand

ARTICLE INFO

Article history:
Received 14 October 2010
Received in revised form
13 December 2010
Accepted 17 December 2010
Available online 25 December 2010

Keywords:
Immunomagnetic particles
Poly(glycidyl methacrylate)
Anti-CD4 monoclonal antibody
CD4$^+$ lymphocyte separation

ABSTRACT

Novel immunomagnetic particles have been prepared for separation of CD4$^+$ lymphocytes. The magnetic nanoparticles with a diameter of approximately 5–6 nm were first synthesized by co-precipitation from ferrous and ferric iron solutions and subsequently encapsulated with poly(glycidyl methacrylate) (PGMA) by precipitation polymerization. Monoclonal antibody specific to CD4 molecules expressed on CD4$^+$ lymphocytes was conjugated to the surface of magnetic PGMA particles through covalent bonding between epoxide functional groups on the particle surface and primary amine groups of the antibodies. The generated immunomagnetic particles have successfully separated CD4$^+$ lymphocytes from whole blood with over 95% purity. The results indicated that these particles can be employed for cell separation and provide a strong potential to be applied in various biomedical applications including diagnosis, and monitoring of human diseases.

1. Introduction

CD4$^+$ lymphocytes are leukocytes that play a central role in the body's immune system. They function as coordinators of the immune responses that assist B lymphocytes in the production of antibody, as well as in augmenting cellular immune responses to defeat pathogens [1]. For therapeutic approach, purification of CD4$^+$ lymphocytes can be used in adoptive cellular therapy for various diseases [2–4]. As CD4$^+$ lymphocytes are the target for human immunodeficiency virus (HIV), currently, number of circulating CD4$^+$ lymphocytes are the most common surrogate marker for monitoring disease progression and therapy in HIV infection [5,6]. Therefore, development of material, technology, and methodology for specific separation of CD4$^+$ lymphocytes is indispensable.

Among the current cell separation techniques, magnetic cell separation technique has received much attention since it provides many advantages over other methods as it is less time consumable, cost-effective, and high specificity [7–9]. The two key magnetic components of such systems are the magnetic particles used in the separation of the biological entities, and the magnetic field used to separate them [10].

For magnetic particles, monodispersity, high magnetization, stability in physiological salinity, and CD4-affinity targeting of magnetic particles are crucial. Since the naked magnetic particles are sensitive to air and aggregate easily due to their magneto–dipole interparticle interaction, surface-protective layers are required to protect them from oxidation and to magnetically isolate individual particles. In particular, polymer shell provides both steric and electrostatic stabilization in physiological medium and protects the leakage of magnetic particles. Moreover, polymers with abundant functional groups, e.g. amine, carboxylate, and thiol groups, are of great interest as they can covalently conjugate with protein of interest. From this viewpoint, poly(glycidyl methacrylate) (PGMA) can be an excellent candidate. Since PGMA possess the reactive epoxide functional groups, which can be directly coupled with biomolecules via their ring opening reactions and further modified with various functional groups. In addition, this conjugation takes place easily at room temperature without an addition of activator and/or cross-linker. Several methods on preparation of magnetic PGMA particles have been proposed in the literature including dispersion [11–13], suspension [14–16], and emulsion [17] polymerization. Nonetheless, the methods described above require stabilizer and/or surfactant, which may further interfere with the biomolecule con-

* Corresponding author at: National Nanotechnology Center, 113 Thailand Science Park, Pahonyothin Rd., Klong 1, Klong Luang, Pathumthani 12120, Thailand. Tel.: +66 2564 7100x6551; fax: +66 2564 6981.
** Corresponding author at: Division of Clinical Immunology, Departemnt of Medical Techology, Faculty of Associated Medical Sciences, Chiang Mai Univerisity, Chiang Mai 50200, Thailand. Tel.: +66 53945070; fax: +66 53216424.
E-mail addresses: Nuttaporn@nanotec.or.th (N. Pimpha), Watchara@chiangmai.ac.th (W. Kasinrerk).

0039-9140/$ – see front matter © 2010 Elsevier B.V. All rights reserved.
doi:10.1016/j.talanta.2010.12.032

jugation or cause nonspecific binding in biological application. Magnetic polymer microspheres prepared by swelling and penetration process have also been disclosed [18,19]. Despite the success of this approach, there are still some drawbacks with respect to tedious multiple step reactions and the use of large amounts of toxic organic solvents. Therefore, it is practically necessary to develop convenient, economic and efficient methods for the preparation of magnetic particles containing high fraction of reactive surface functional groups for further covalently conjugation without the use of stabilizer and surfactant.

Recently, two major types of magnetic cell isolation technology, column-based and tube-based systems, have been described. The column-based technology utilizes nano-sized magnetic particles and therefore requires the passing of the labeled cells through a magnetized iron-mesh column to increase cell-capture capacity. The tube-based system generally utilizes micron-sized beads and requires a magnet block for cell separation. Importantly, the strength of the magnetic field required for cell separation differs depending on the size of the magnetic particles [20]. For the micron-sized beads, a simple magnet block which generates field gradients in the order of 1–6 T m^{-1} across 15–50 mL test tube is required. In contrast, the nano-sized beads need high-gradient magnet separators (10–100 T m^{-1}) [10].

Although many types of commercially available magnetic particles have been utilized for $CD4^+$ lymphocytes separation [21,22], the development of magnetic systems to enhance the specificity and separation efficiency is a challenge. Based on antibody–antigen affinity, the utilization of commercial anti-mouse CD4 conjugated magnetic nanoparticles with column and a microfluidic device provided the CD4 separation efficiency in the range of 85–91% [23,22] and 10–91% [21], respectively. Alternatively, according to streptavidin–biotin interaction, synthetic streptavidin-coated magnetic systems for the purification of $CD4^+$ lymphocytes were also developed. Novel streptavidin-functionalized silicon nanowire arrays showed 87.6% separation efficiency [24]. The streptavidin-FITC-conjugated core–shell Fe_3O_4–Au nanocrystals provided only 57% separation, which was proposed to be due to weak magnetic field and incomplete binding of streptavidin conjugated magnetic nanoparticles to biotinylated CD4 cells [25].

To develop an efficient magnetic system for separation of $CD4^+$ lymphocytes, we design simple, specific, and cost-effective CD4 separation system without the need for column separation technique. Magnetic PGMA particles were successfully prepared through a two-stage reaction: (1) preparation of iron oxide nanoparticles, and (2) synthesis of the iron oxide-encapsulated PGMA particles via the precipitation polymerization. Monoclonal antibody specific to CD4 molecules expressed on $CD4^+$ lymphocytes [26,27] was covalently conjugated with epoxide group on the surface of the iron oxide-encapsulated PGMA particles. The efficiency and specificity of using the immunomagnetic particles in $CD4^+$ lymphocyte separation from whole blood were evaluated. Concentration of coated antibodies was also optimized in order to maximize the separation efficiency.

2. Experimental

2.1. Materials

Ferrous chloride tetrahydrate ($FeCl_2{\cdot}4H_2O$, Fluka), ferric chloride hexahydrate ($FeCl_3{\cdot}6H_2O$, Fluka), oleic acid (Merck), acetonitrile (Carlo erba), and ammonium hydroxide solution (40%, w/w, Merck) were used as received. Monomers, glycidyl methacrylate (GMA) and divinylbenzene (DVB), from Merck were purified to remove inhibitors using a column packed with alumina adsorbent. Benzoyl peroxide (BPO) was twice recrystallized from methanol. All other chemicals were commercially available and of analytical grade.

2.2. Preparation of oleic-coated iron oxide nanoparticles (IO)

Iron oxide nanoparticles coated with oleic acid were synthesized by a coprecipitation method. Briefly, $FeCl_2{\cdot}4H_2O$ (1.6 g, 2 M) and $FeCl_3{\cdot}6H_2O$ (4.32 g, 1 M) were dissolved in deionized water (20 mL), then ammonium hydroxide (80 mL, 1.4 M) was added immediately to the mixtures under nitrogen atmosphere at 0–5 °C. After 30 min, the resulting black dispersion was washed repeatedly with deionized water until the pH = 7. Thereafter, the collected nanoparticles were dispersed in 0.01 M HCl and further refluxed in the presence of oleic acid (100 mL) for an hour. The black iron oxide nanoparticles were then purified by decantation and redispersed in cyclohexane. Finally, the nanoparticles were prepared at concentration of 20 mg/mL for the subsequent experiments.

2.3. Preparation of IO-encapsulated poly(glycidyl methacrylate) (PGMA) particles

The IO-encapsulated PGMA particles were prepared by precipitation polymerization of GMA monomer in acetonitrile medium. One milliliter of synthesized IO (20 mg) was dispersed thoroughly with GMA and DVB comonomers, using sonication for 5 min. The IO dispersions were subsequently introduced to the acetonitrile medium in 100 mL of round bottom flask. The BPO initiator was also added in the mixtures. The concentration of GMA mixed with DVB was set at 6 wt% for acetonitrile medium. The mole ratio of GMA and DVB was constant at 50:50 mol%. While the BPO initiator was fixed at 4 wt% for the comonomers added. After completing the ingredients preparation, the polymerizing mixtures were purged with N_2 for 30 min and then placed into the shaking incubator with an agitation speed of 250 rpm at 70 °C for starting the polymerization reaction. The reaction was continued for 24 h. The resulted particles were purified by decantation (Nd–Fe–B permanent magnets, ~0.18 T) and washed with methanol and water, respectively. For comparison, the PGMA particles without IO were prepared under the same condition and further purified by a repeated centrifugation. Finally, the particles were prepared at concentration of 1×10^7 beads/mL for subsequent experiments.

2.4. Characterization

Morphology and particle size of IO were observed with a transmission electron microscope in both normal transmission and high-resolution modes (TEM and HRTEM, JEM-2010, JEOL) at an acceleration voltage of 200 kV. The crystallographic structures of both IO and IO-encapsulated PGMA particles were studied with X-ray diffraction spectroscopy (XRD, RIGAKU TTRAX III) equipped with CuK_α radiation (λ = 0.15418 nm). The 2θ range used in the measurement was 20–70° in step of 0.02°. The powder sample was obtained by drying under vacuum and grinding to fine powder. The average crystallite size was estimated using the Debye–Scherrer equation:

$$D = \frac{K\lambda}{\beta \cos \theta} \quad (1)$$

where D is the average crystal diameter, β is the corrected peak width (full width at half-maximum), K is a constant related to the shape of the crystallites, about 0.9 for magnetite, λ is the wavelength of the X-ray employed, and θ is the diffraction angle. The width of the diffraction peak with the highest intensity was selected for the calculation.

The size and morphology of IO-encapsulated PGMA particles were observed with scanning electron microscope (SEM, S-2500, Hitachi, Japan). To prepare the specimen, a particle dispersion (10 mg/mL) was dropped on a cover glass and dried in a dust-free environment. The dried specimens were stuck on the sample holders with a double-coated carbon conductive tab and then were sputter-coated under vacuum with platinum and palladium using a sputter coater (E-102, Hitachi, Japan). The sputter-coated specimens were then observed by the microscope at 15 kV. Fourier-transform infrared measurement (FTIR) was performed in an attenuated total reflection (ATR) mode using an FTIR spectrophotometer (Equinox 55, Bruker), equipped with a single reflection ATR unit. The dried samples were pressed in contact between the internal reflection element (IRE) crystal and the gripper plate. The resolution of 4 cm^{-1} at 32 scans was used. The scanning for each spectrum was done in the range between 4000 and 600 cm^{-1}. Thermogravimetric analysis (TGA) was employed for the measurement of the IO content (wt%) using a thermogravimetric analyzer (TGA/SDTA851, Mettler). The sample of 5–10 mg was accurately weighed into an aluminum pan. The measurement was conducted at a heating rate of 10 °C/min under nitrogen purge at 20 mL/min. Compositions of IO in PGMA particles were calculated based on the following equation. The residue weight is the weight of materials remaining at 650 °C.

$$\text{Composition}\,(\%) = \frac{\text{Weight of residue}}{\text{Weight of dried particle}} \times 100 \quad (2)$$

The magnetic properties were investigated using room temperature vibrating sample magnetometer (VSM, Lakeshore 7400, Lakeshore) at an applied maximum field of 10,000 G. Flow cytometry analysis was performed on a FACSort flow cytometer (Becton Dickinson, San Jose, CA).

2.5. Anti-CD4 monoclonal antibody conjugation

To conjugate anti-CD4 monoclonal antibody on the magnetic particle, direct conjugation method described elsewhere [26] was carried out. Briefly, an anti-CD4 monoclonal antibody (mAb), named MT4 (IgM isotype), specific recognized CD4 molecules expressed on $CD4^+$ lymphocytes was used in this study. Production and purification of mAb MT4 were described elsewhere [26]. IO-encapsulated PGMA particles were washed 3 times with 0.1 M phosphate buffer pH 7.4 (PB) and decanted using a magnetic particle concentrator (MPC Dynal, Invitrogen, Oslo, Norway). The particles were then adjusted to 1×10^6 particles with PB. Various concentrations of purified mAb MT4 (0, 2, 10, 20, and 40 μg) were added to 500 μL particle suspension. The mixtures were rotated at 4 °C for 6 h. Then, 500 μL of 2% bovine serum albumin (BSA) in phosphate-buffered saline (PBS) containing 0.02% sodium azide (2% BSA–PBS–0.02% NaN_3) was added in order to block the residual active epoxide functional groups on the surface of particle. The particles were rotated at 4 °C for another 16–20 h. Afterward, the particles were washed 3 times with PBS to remove unbound mAb MT4. The washed beads were concentrated to 1×10^6 beads/500 μL in 1% BSA–PBS–NaN_3 for subsequent experiments.

2.6. Evaluation of the mAb MT4 conjugated immunomagnetic particles

To determine the presence of mAb MT4 on the immunomagnetic PGMA particles, the MT4 coated immunomagnetic particles (50 μL) were mixed with 50 μL of phycoerythrin (PE)-conjugated goat anti-mouse IgG or PE-conjugated goat anti-mouse IgM antibodies (Beckman Coulter Inc., Brea, CA, USA). The mixture was incubated at room temperature for 30 min in dark. Thereafter, the immunomagnetic PGMA particles were magnetically washed with the PBS three times and redispersed in 1% BSA–PBS–NaN_3. The fluorescence of the particles was evaluated by a flow cytometer (Becton Dickinson).

2.7. Magnetic $CD4^+$ lymphocyte separation

Whole blood samples were obtained from healthy donors using vacutainer tubes (BD Biosciences, San Jose, CA, USA) containing tripotassium ethylenediaminetetraacetic acid (K_3EDTA). Two hundred microliter of K_3EDTA whole blood were pipetted into 3 separated tubes, tube A (un-treated blood control), tube B (negative control), and tube C (test). Two hundred microliters of PBS were added into tube A, 200 μL of the BSA-blocked un-conjugated magnetic PGMA particles (4×10^5 particles) were added into tube B, and 200 μL of the mAb MT4-immunomagnetic PGMA particles (4×10^5 particles) were added into tube C. The tubes were rotated at room temperature for 30 min. Thereafter, the tubes were placed on a magnetic particle concentrator (MPC Dynal, Invitrogen) for 5 min for depletion of $CD4^+$ lymphocytes. One hundred microliters of the $CD4^+$ lymphocyte depleted blood were collected and incubated at room temperature in dark with 20 μL of CD3-FITC/CD4-PE/CD45-PerCP reagent (Tritest™ three color reagent; BD Biosciences). After 15 min incubation at room temperature, 1 mL of lysing solution (PBS pH 7.2, diethylene glycol 3 mmol, formaldehyde 37%) was added, and the samples were allowed to stand at room temperature in the dark for 10 min. Cells were then washed twice with PBS, followed by fix with 1% paraformaldehyde in PBS, and analysed by a flow cytometer using Cellquest software (Becton Dickinson). The percentages of $CD4^+$ lymphocytes in the total lymphocyte population in all tested tubes were determined. The reproducibility of the results was confirmed through triplicate experiments.

3. Results and discussion

In designing magnetic cell separation system, the two key magnetic components, magnetic particles and the magnetic field used to separate them, are needed to be concerned. In this present study, micron-sized particles were developed in order to facilitate the ease of particle detection and cell separation. Magnetic PGMA particles were successfully prepared through a two-stage reaction: (1) preparation of iron oxide nanoparticles, and (2) synthesis of the iron oxide-encapsulated PGMA particles via the precipitation polymerization. In general, the preparation of PGMA particles require stabilizer and/or surfactant, which may further interfere with the biomolecule conjugation or cause nonspecific binding in biological applications. In addition, it involves tedious multiple step reactions with the use of large amounts of toxic organic solvents. Compared with current preparation techniques, our synthetic strategy is simple and efficient for the preparation of magnetic particles containing high fraction of reactive surface functional groups for further covalently conjugation without the use of stabilizer and surfactant. Moreover, the epoxide groups on the surface of PGMA particles allow direct labeling with antibody through covalent bonding without addition of significant sample preparation process.

Monoclonal antibody specific to CD4 molecules expressed on $CD4^+$ lymphocytes was covalently conjugated with epoxide group on the surface of the iron oxide-encapsulated PGMA particles. The efficiency and specificity of using the immunomagnetic particles in $CD4^+$ lymphocyte separation from whole blood were evaluated. Fig. 1 illustrates synthetic scheme of iron oxide-encapsulated PGMA particles and their application for $CD4^+$ lymphocyte separation from whole blood.

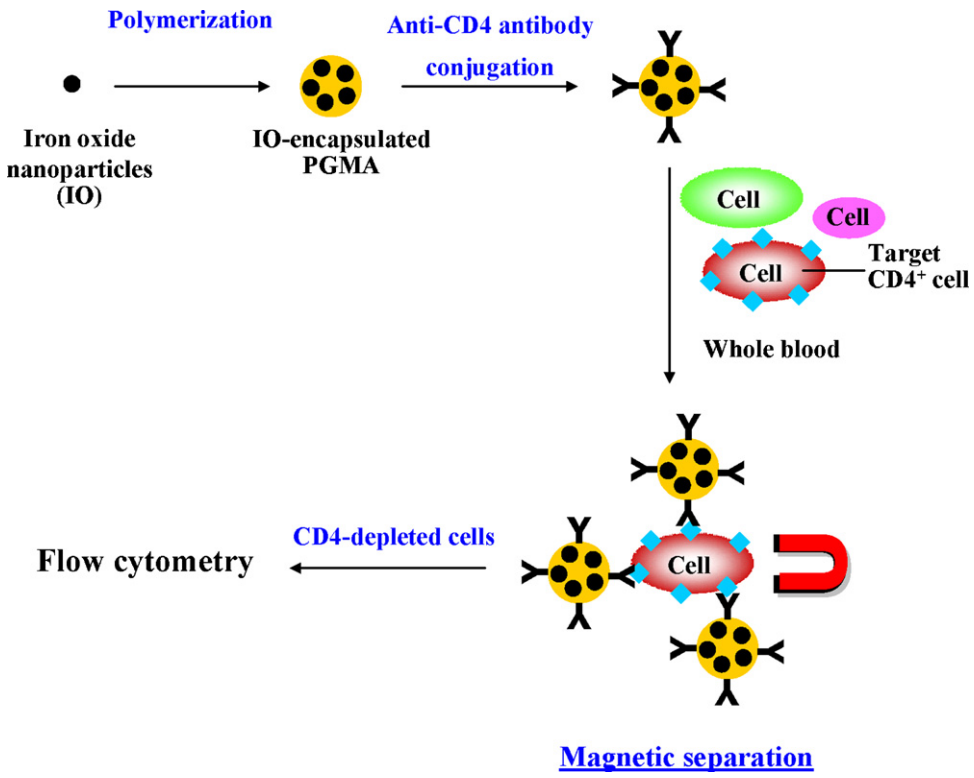

Fig. 1. Synthetic scheme of iron oxide-encapsulated PGMA particles and their application for $CD4^+$ lymphocyte separation from whole blood.

3.1. Preparation of oleic-coated iron oxide nanoparticles (IO)

The iron oxide nanoparticles were synthesized from the coprecipitation of Fe^{2+} and Fe^{3+} ions in an aqueous solution upon the addition of ammonium hydroxide [28]. In this study, oleic acid was applied to stabilize the obtained iron oxide nanoparticles through the reaction between carboxylic acid groups and the hydroxyl groups on the iron oxide nanoparticle surface leading to coagulation prevention. Moreover, hydrophobic long alkyl chain oleic acid on the iron oxide nanoparticle surface also facilitates the hydrophobic compatibility between the nanoparticle and the monomer in the following polymerization step.

The crystal structure and phase purity of the obtained oleic-coated iron oxide nanoparticles (IO) were determined by XRD as shown in Fig. 2a. The data for IO exhibited the diffraction peaks, which can be assigned to (2 2 0), (3 1 1), (4 0 0), (5 1 1), and (4 4 0) planes of spinel phase Fe_3O_4 (JCPDS 87-2334). The mean particle diameters were calculated to be 8.3 nm from the XRD pattern based on the half-height of the (3 1 1) diffraction peak using Scherrer equation.

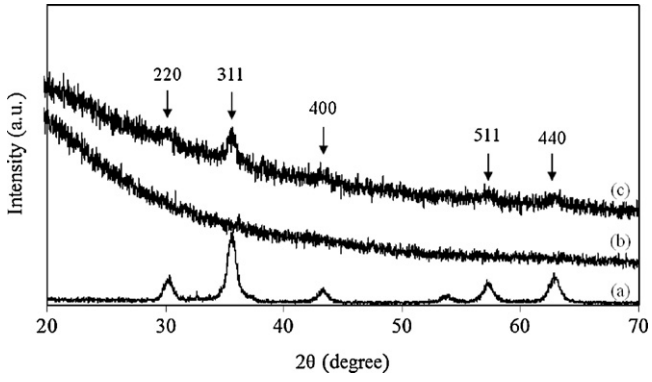

Fig. 2. Comparison of XRD patterns of (a) oleic-coated iron oxide nanoparticles; (b) poly(glycidyl methacrylate) particles; and (c) iron oxide-encapsulated poly(glycidyl methacrylate) particles.

Particle size analysis was also determined by TEM, as shown in Fig. 3a. IO displayed spherical shape with uniform distribution. Measuring the diameter of 100 randomly selected nanoparticles in enlarged TEM images resulted in the particle size distribution histogram shown in Fig. 3b. The size distribution was found to be narrow and an average size of 7–8 nm, which is in accordance with the values observed by XRD calculation. HRTEM image was presented in Fig. 3c showing that IO had high crystallinity and the distinct lattices.

Magnetic behavior at room temperature was evaluated by VSM. Fig. 4a shows a typical plot of magnetization versus applied magnetic field (hysteresis curve). The synthesized IO revealed a superparamagnetic behavior, as evidenced by zero coercivity and remanence on the magnetization loops. The saturated magnetization (Ms) of IO was about 54 emu/g, which is comparable to IO produced by other methods [29,30].

The presence of olelate coating on the surface of nanoparticles was confirmed by FTIR (shown in Fig. 5a). The absorption peaks at 1700 cm^{-1} related to the C=O stretching vibration of oleic ester, and 539 cm^{-1} attributed to the Fe–O stretching were clearly observed.

3.2. Preparation of IO-encapsulated PGMA particles

Monodisperse PGMA particles were synthesized using a precipitation polymerization of glycidyl methacrylate and divinylbenzene in acetonitrile medium without any added surfactant or stabilizer. The possible mechanism reaction to form PGMA particles was proposed by Choe et al. [31]. For the preparation of IO-encapsulated PGMA particles, the hydrophobic oleate coating of IO nanoparticles, which is compatible with GMA monomers, would facilitate the encapsulation leading to the entrapment of IO in PGMA particles. In addition, the epoxide group on the surface would react easily with

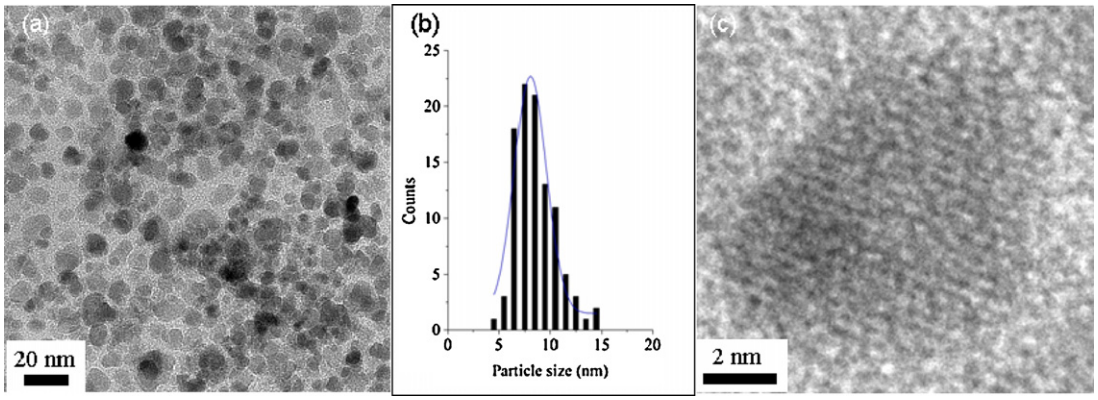

Fig. 3. TEM analysis of oleic-coated iron oxide nanoparticles. (a) Morphology, (b) corresponding size distribution of oleic-coated iron oxide nanoparticles, and (c) lattice image.

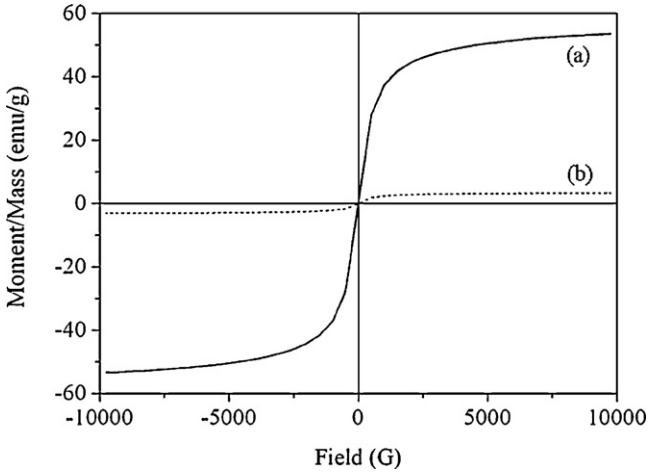

Fig. 4. Room temperature magnetization hysteresis curves of (a) oleic-coated iron oxide nanoparticles, and (b) iron oxide-encapsulated poly(glycidyl methacrylate) particles.

various nucleophiles and thus allow the subsequent functionalize by ring opening epoxide with any protein of interest.

The FTIR was employed to characterize the chemical functional groups present in the IO-encapsulated PGMA particles compared with IO and original PGMA particles. The FTIR spectrum of IO-encapsulated PGMA particles (Fig. 5c) was similar to the original

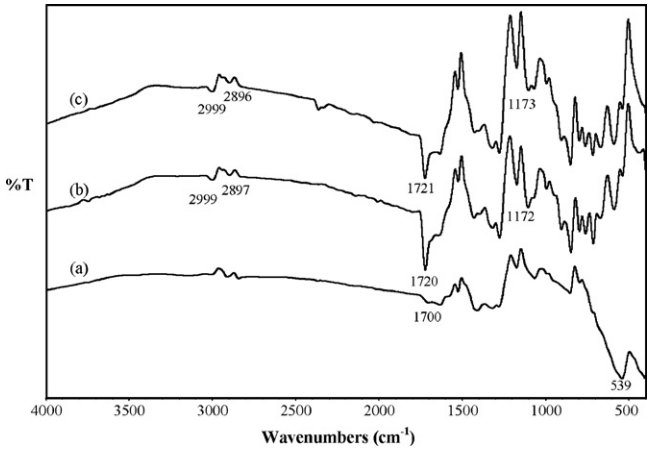

Fig. 5. Comparison of FTIR spectra of (a) oleic-coated iron oxide nanoparticles, (b) poly(glycidyl methacrylate) particles, and (c) iron oxide-encapsulated poly(glycidyl methacrylate) particles.

PGMA particles (Fig. 5b). The formation of characteristic peaks at 1720 and 1172 cm^{-1} corresponded to C=O and C–O stretching vibrations of ester groups from glycidyl methacrylate molecule, indicating the presence of epoxide groups. The peaks at 2896 and 2999 cm^{-1} were attributed to symmetric and asymmetric C–H stretching vibrations. Although the characteristic peaks of IO (stretching vibration of C=O groups of oleic ester, 1700 cm^{-1} or Fe–O, 539 cm^{-1}) were not observed in the spectrum of IO-encapsulated PGMA particles, magnetic property and XRD data (will be discussed later) provided the convincing evidence for IO encapsulation.

XRD analysis of the IO-encapsulated PGMA particles revealed the diffraction peaks corresponded to IO (Fig. 2c), while no that characteristic peaks of IO were observed in original PGMA particles (Fig. 2b). This indicated that IO was successfully encapsulated in PGMA particles. The magnetic properties were evaluated by VSM. Fig. 4b shows the magnetization hysteresis curve of the IO-encapsulated PGMA particles. The original PGMA particles were nonmagnetic (data not shown), whereas the IO-encapsulated PGMA particles exhibited superparamagnetic properties at room temperature as no hysteresis loop was observed. The Ms of IO-encapsulated PGMA particles was about 3.25 emu/g. Reduction of Ms after encapsulation corresponded to many reports [32–34] that the composite IO were stabilized with polymers could result in the reduction of the magnetic properties of IO due to the presence of the diamagnetic components. Therefore, this is commonly employed for the reduction of magnetic properties of the obtained IO-encapsulated PGMA particles.

Fig. 6 shows the scanning electron microscope (SEM) micrographs of the original PGMA and IO-encapsulated PGMA particles. Apparently, the original PGMA particles had spherical shape with uniform size distribution (Fig. 6a). The average diameter was around 3 μm. Encapsulation of IO resulted in coagulum form with larger size up to 30 μm (Fig. 6b). The rationale for these changes could possibly due to an agglomeration of particle through the strong magneto–dipole interaction exerted between the particles [35]. The coagulation also indicates that although the DVB provide a strong effect on colloidal stability without stabilizer, this effect might not effective enough to prevent the particle from flocculating together under the presence of IO. In addition, the size of IO-encapsulated PGMA particles can be controlled by varying the concentration of DVB monomer. Increasing in DVB concentration resulted in the smaller size of the particles.

Fig. 7 represents the TGA thermograms of the original PGMA and IO-encapsulated PGMA particles. The weight loss in the first step (25–200 °C) was attributed to the vaporization of small molecules such as acetonitrile and low-molecular-weight polymer. The second weight loss observed at temperatures higher

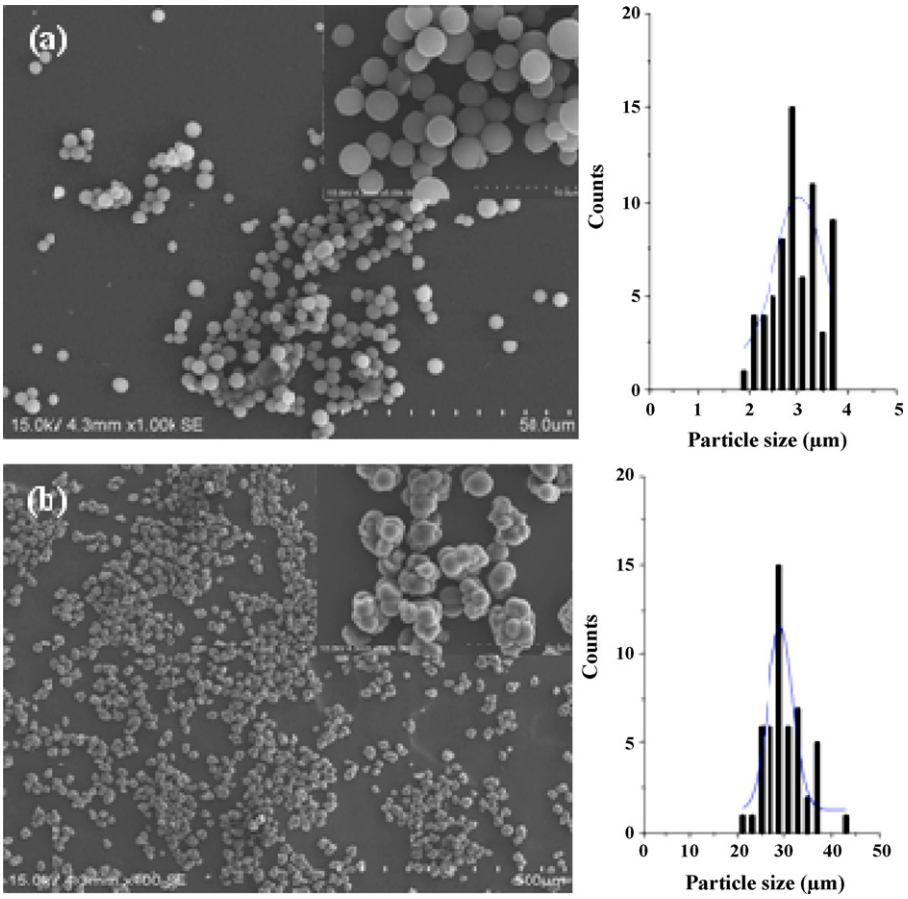

Fig. 6. SEM images showing morphology and size distribution of (a) poly(glycidyl methacrylate) particles, and (b) iron oxide-encapsulated poly(glycidyl methacrylate) particles.

than 200 °C was corresponded to the slow decomposition of the higher-molecular-weight species present in the particles. The composition of IO in PGMA particles was also evaluated by determining the remaining IO fractions. The encapsulated percentage of IO in the particles was 9.2%.

3.3. Anti-CD4 monoclonal antibody conjugation

In order to target CD4 molecules expressed on $CD4^+$ lymphocytes, surface modification of IO-encapsulated PGMA particles with anti-CD4 antibody is essential. Although direct adsorption of the antibody molecules to the particle surface through electrostatic interaction is possible, there are still some drawbacks with respect to protein denature and/or steric hindrance. To address this problem, covalent conjugation of antibodies to the IO-encapsulated PGMA particles has been proposed in this present study. Additionally, the covalent conjugation would provide the right orientation of the attached antibodies exposing the binding sites available for target biomolecules.

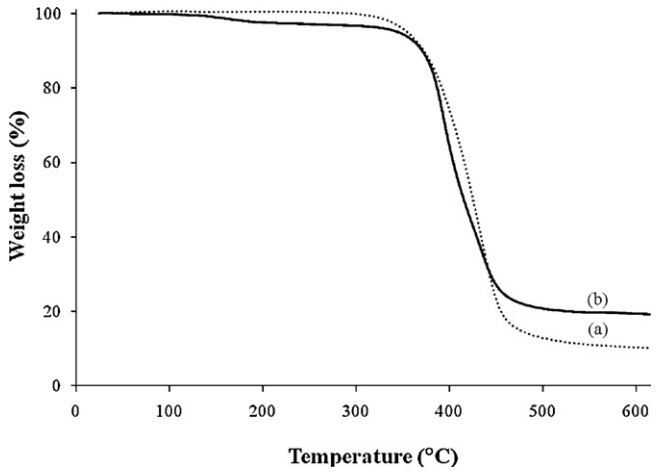

Fig. 7. TGA thermograms of (a) poly(glycidyl methacrylate) particles, and (b) iron oxide-encapsulated poly(glycidyl methacrylate) particles.

An anti-CD4 mAb, named MT4 which is IgM isotype, was generated in our laboratory. The mAb MT4 was demonstrated to restricted react with CD4 proteins expressed on $CD4^+$ lymphocytes [26,27]. In this study, purified mAb MT4 was conjugated with IO-encapsulated PGMA particles to generate immunomagnetic PGMA particles and subsequently used in $CD4^+$ lymphocyte separation. The mAb MT4 was attached to the surface of IO-encapsulated PGMA particles through covalent bonding between epoxide functional groups on the surface of particle and primary amine groups of antibody.

To monitor the presence of mAb MT4 on the surface of immunomagnetic PGMA particles, the as-prepared particles were stained with PE-labeled anti-mouse IgM antibody (PE-αIgM) and analysed by flow cytometry as shown in Fig. 8. For comparison, unmodified IO-encapsulated PGMA particles were investigated as negative control. The immunomagnetic PGMA particles showed strong fluorescent signal, while that of unmodified particles had very low fluorescence signal. The fluorescence signal attributes to specific reaction between anti-IgM conjugate and the IgM molecules bound on PGMA particle surface. These data indicated that mAb MT4 was successfully functionalized on the surface of the magnetic

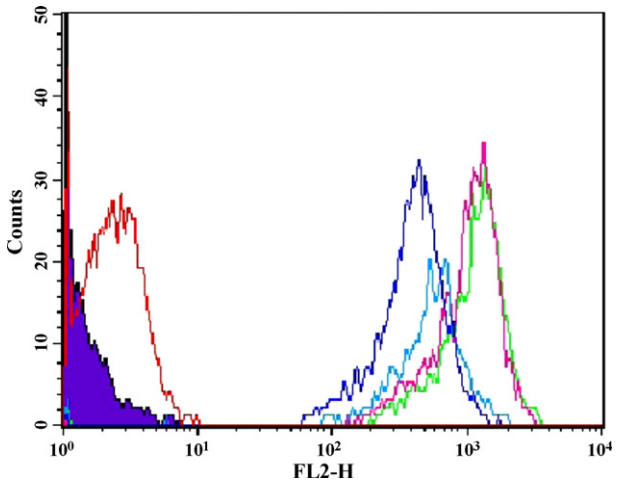

Fig. 8. Evaluation of the conjugation of anti-CD4 monoclonal antibody (mAb MT4) to the magnetic particles by immunofluorescent staining and flow cytometry. The mAb MT4-conjugated and un-conjugated particles were stained with phycoerythrin (PE)-labeled anti mouse (α) IgM and IgG antibody. The stained particles were analysed by flow cytometer and gated according to their size and granularity. Key: PE-αIgM + un-conjugated magnetic particles ( ); PE-αIgM + conjugated immunomagnetic particles at mAb MT4 concentrations of 2 ( ), 10 ( ), 20 ( ), and 40 μg ( ); and PE-αIgG + conjugated immunomagnetic particles at mAb MT4 concentration of 20 μg ( ).

PGMA particles, without the signs of denaturation or degradation. The immunomagnetic PGMA particles were also examined using PE-labeled anti-mouse IgG (PE-αIgG) instead of their specific conjugate, PE-αIgM. The fluorescent signal obtained from using PE-αIgG conjugate was very low.

Although the used chemical coupling method provided the random orientation of the antibodies, in our experiments, we demonstrated the high separation efficiency. Our results indicated that the proper orientation of anti-CD4 monoclonal antibodies was occurred on the particles and generated the binding of CD4 molecule expressed on $CD4^+$ lymphocytes.

The optimum concentration of mAb MT4 for coating on the immunomagnetic PGMA particles has been evaluated. As shown in Fig. 8, increasing in mAb MT4 concentration from 2 to 20 μg increased the fluorescent intensity; however, further increasing over 40 μg resulted in weaker fluorescent signal. This effect could possibly due to steric hindrance of the coated antibodies.

3.4. Magnetic $CD4^+$ lymphocyte separation

$CD4^+$ lymphocytes are a sub-population of T lymphocytes which expressing CD4 molecules on their surface. These cells provide helper function in adaptive immunity [1]. $CD4^+$ lymphocytes have been widely applied to modulate the immune system in both animals and human [2–4]. In addition, quantitative analysis of $CD4^+$ lymphocytes is one of the crucial steps for treatment and management of immunodeficiency diseases and HIV infection [5,6,26]. The generated immunomagnetic PGMA particles were then validated for their ability in binding and separation of $CD4^+$ lymphocytes.

In this study, the generated immunomagnetic PGMA particles were first incubated with whole blood sample. As the antibody coated magnetic particles were directly added into whole blood which contain large amount of immunoglobulins, the Fc receptors expressed on leukocytes are not affecting or non-specific binding to the antibody coated on the particles. In this step, the immunomagnetic particles bound specifically to $CD4^+$ lymphocytes according to the specific antigen–antibody interactions. Then, the magnetic particles bound $CD4^+$ lymphocytes were removed magnetically out from the blood sample. Consequently, the $CD4^+$ lymphocytes depleted blood was analysed by flow cytometry and the percentage of the residue lymphocytes was determined. In parallel, the same blood sample, but without addition of immunomagnetic PGMA particles, was also analysed for the percentage of total $CD4^+$ lymphocytes. Fig. 9 shows flow cytometry results comparing of the untreated and immunomagnetic treated bloods. The percentage of the total $CD4^+$ lymphocytes in whole blood sample, before $CD4^+$ lymphocyte depletion, was (mean ± S.D.) 35 ± 4% (Fig. 9a). In immunomagnetic PGMA particle treatment (using 10 μg of mAb MT4 conjugation), the number of $CD4^+$ lymphocytes was reduced to 2 ± 0.5% (Fig. 9b). These results indicated that the immunomagnetic PGMA particles bound to $CD4^+$ lymphocytes and the $CD4^+$ lymphocytes were successfully pulled out from the whole blood with exterior permanent magnet. In comparison, un-conjugated magnetic PGMA particles showed 35 ± 4% of $CD4^+$ lymphocytes which was the same as those obtained from un-treated blood (data not shown). When the percentage of separation efficiency was calculated ($n = 3$), immunomagnetic PGMA particles provided 95 ± 3% separation efficiency.

The effect of mAb MT4 concentration on separation efficiency was also studied as shown in Fig. 10. The immunomagnetic PGMA particles coating with 2, 10, 20, and 40 μg of mAb MT4 showed

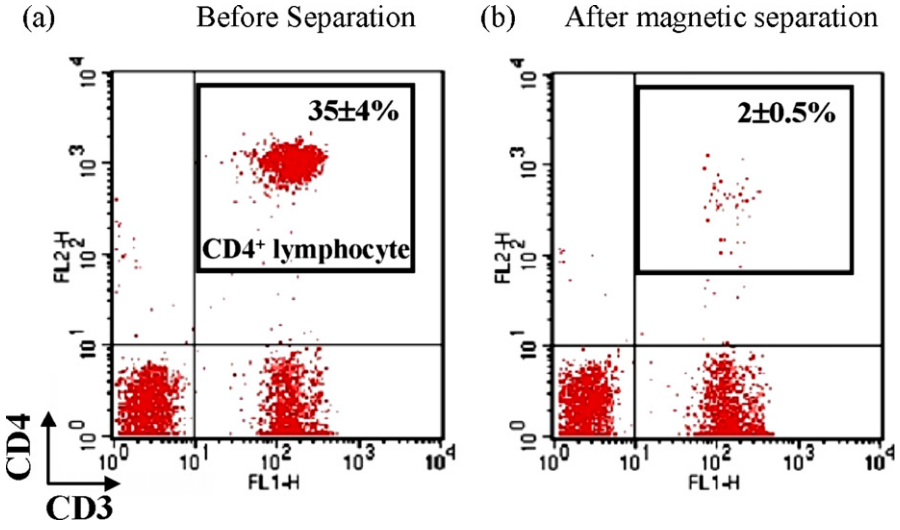

Fig. 9. Separation of $CD4^+$ lymphocytes by anti-CD4 mAb conjugated magnetic particles. Whole blood sample was incubated with un-conjugated magnetic particles (a) or mAb MT4 conjugated immunomagnetic particle (b). Magnetic particle bound cells were magnetically depleted and the $CD4^+$ lymphocytes in the depleted blood were determined by flow cytometry. The results are representative of three independent experiments.

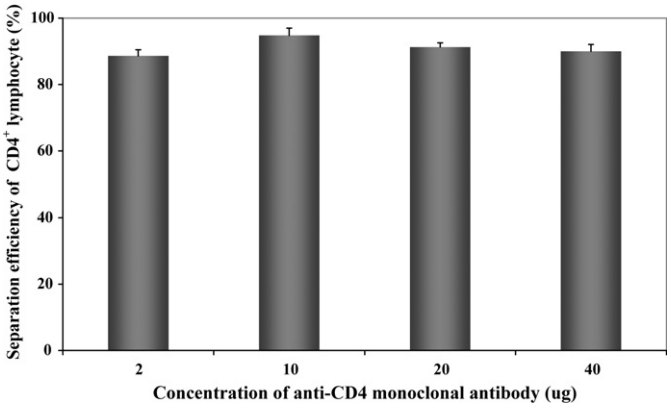

Fig. 10. Cell separation efficiency of anti-CD4 mAb conjugated magnetic particles at concentration of 2, 10, 20, and 40 μg. No statistical significant difference of the $CD4^+$ lymphocyte separation efficiency was observed at all concentrations of antibody tested.

89 ± 2, 95 ± 3, 93 ± 2, and 91 ± 3% depletion of $CD4^+$ lymphocytes, respectively. All mAb MT4 concentrations provided an acceptable value (>90% depletion). The immunomagnetic PGMA particles coated with 10 μg of mAb MT4 was the most effective for CD4 separation. The CD4 separation efficiency of PGMA particles coated with 40 μg was lower than those of 20 and 10 μg could presumably due to the steric hindrance of the coated antibodies similar to the work of Neurauter et al. [20].

As the magnetic cell separation efficiency strongly depends on magnetophoretic mobility, choice of targeted-specific receptors, and separation conditions [10], the immunomagnetic PGMA particles have three distinct advantages over the current magnetic CD4 separation systems. First, the epoxide groups on the surface of PGMA particles allow direct labeling with antibody through covalent bonding without significant sample preparation process. This chemical bonding could limit the non-specific binding as well as provide stable antibody–bead conjugates upon drag force acting on the moving cell. Second, as the lymphocyte cell-size is in the micrometer range, the use of micron-sized PGMA particles could facilitate the interaction between particle-cell. A larger cell will exhibit a larger friction coefficient, thus, the drag force on a larger cell will be greater. The utilization of the micro-sized particles can possess a higher magnetic moment comparing with nanoparticles, therefore, enhancing magnetophoretic mobility and reducing separation time [10,36]. Another advantage is the utilization of highly specific monoclonal antibody (purified mAb MT4) toward $CD4^+$ lymphocyte. Conjugating mAb MT4 onto PGMA particles does not adversely affect their binding properties with intact cells, and therefore, they can be employed for selective extraction and sensitive molecular detection.

The utilization of micron-sized PGMA particles in this assay was possible only because there are sufficient CD4 binding sites. For the analysis of cells having few recognition sites, small particles are superior in terms of accessible surface and higher mass transfer kinetics [37].

It can be concluded that the immunomagnetic PGMA particle described in our manuscript offers rapid and direct access to target $CD4^+$ lymphocyte from whole blood without the need for column separation techniques and centrifugation. The immunomagnetic PGMA particles provide the high separation efficiency due to the high reactivity of the epoxide functional groups on the surface of particle which facilitate the direct bioconjugation and the presence of the high specificity of monoclonal antibody. Therefore, the generated immunomagnetic PGMA particles can be useful for separation of $CD4^+$ lymphocytes for monitoring HIV diseases progression and efficiency of antiretroviral treatment [26]. Moreover, the magnetic PGMA particles platform can be applied to the separation of a wide variety of cells, including leukocytes, tumors, or stem cells by changing the ligand that specific to the marker on the targeted cell surface. The developed cell separation strategy can be applied to various biomedical applications including treatment, diagnosis, and monitoring of diseases.

4. Conclusions

Magnetic PGMA particles were successfully prepared through a two-stage reaction: (1) preparation of iron oxide nanoparticles, and (2) synthesis of the iron oxide-encapsulated PGMA particles via the precipitation polymerization. Monoclonal antibody specific with CD4 molecules expressed on $CD4^+$ lymphocytes was conjugated on magnetic PGMA particles' surface through covalent bonding between epoxide functional groups on the surface of particle and primary amine groups of antibody. These immunomagnetic PGMA particles were specific and highly efficient in separation of $CD4^+$ lymphocytes from whole blood. Therefore, the generated immunomagnetic PGMA particles can be useful for $CD4^+$ lymphocytes and other cells separation which may be applied to various biomedical applications including treatment, diagnosis, and monitoring of diseases.

Acknowledgements

This research was financially supported from the National Nanotechnology Center, National Science and Development Agency Nanotechnology Center, Thailand and the NSTDA Research Chair Grant, National Sciences and Technology Development Agency (Thailand). K.M. is a Ph.D student of the Biomedical Sciences program, Faculty of Associated Medical Sciences, Chiang Mai University.

References

[1] A.K. Abbas, A.H. Lichtman, Cellular and Molecular Immunology, 5th ed., Saunders, Philadelphia, 2003.
[2] S.A. Grupp, C.H. June, Curr. Top. Microbiol. Immunol. (2010) (Aug 11, Epub ahead of print).
[3] E. Klyuchnikov, A. Sputtek, O. Slesarchuk, M. Lioznov, T. Stübig, U. Bacher, G. Amtsfeld, E. Merle, M.L. Reckhaus, B. Fehse, C. Wolschke, R. Adjallé, F. Ayuk, A. Zander, N. Kröger, Biol Blood Marrow Transplant. (2010), Jul 14, Epub ahead of print.
[4] C. Carnaud, V. Bachy, Prion 4 (2010) 66.
[5] M. Dybul, A.S. Fauci, J.G. Bartlett, MMWR Recomm. Rep. 51 (2002) 1.
[6] V. De Gruttola, R. Gelman, S. Lagakos, Infect. Agents Dis. 2 (1994) 304.
[7] J.H. Dykes, J. Toporski, G. Juliusson, A.N. Békássy, S. Lenhoff, A. Lindmark, S. Scheding, Transfusion 47 (2007) 2134.
[8] M. Kuhara, H. Takeyama, T. Tanaka, T. Matsunaga, Anal. Chem. 76 (2004) 6207.
[9] A. Thiel, A. Scheffold, A. Radbruch, Immunotechnology 4 (1998) 89.
[10] G.P. Hatch, R.E. Stelter, J. Magn. Magn. Mater. 225 (2001) 262.
[11] D. Horák, E. Petrovský, A. Kapička, T. Frederichs, J. Magn. Magn. Mater. 311 (2007) 500.
[12] M. Omer-Mizrahi, S. Margel, J. Colloid Interface Sci. 329 (2009) 228.
[13] B. Rittich, A. Španová, D. Horák, M.J. Beneš, L. Klesnilová, K. Petrová, A. Rybnikář, Colloid Surf. B 52 (2006) 143.
[14] G. Bayramoğlu, M.Y. Arica, J. Hazard. Mater. 144 (2007) 449.
[15] G. Bayramoğlu, E. Loğoğlu, M.Y. Arica, Colloid Surf. A 297 (2007) 55.
[16] X. Liu, H. Liu, J. Xing, Y. Guan, Z. Ma, G. Shan, C. Yang, China Particuology 1 (2003) 76.
[17] E. Pollert, K. Knížek, M. Maryško, K. Závěta, A. Lančok, J. Boháček, D. Horák, M. Babič, J. Magn. Magn. Mater. 306 (2006) 241.
[18] T.-H. Chung, J.-Y. Chang, W.-C. Lee, J. Magn. Magn. Mater. 321 (2009) 1635.
[19] T.-H. Chung, W.-C. Lee, React. Funct. Polym. 68 (2008) 1441.
[20] A.A. Neurauter, M. Bonyhadi, E. Lien, L. Nøkleby, E. Ruud, S. Camacho, T. Aarvak, Adv. Biochem. Eng. Biotechnol. 106 (2007) 41.
[21] D. Gao, H.-F. Li, G.-S. Guo, J.-M. Lin, Talanta 82 (2010) 528.
[22] S.D. Nielsen, J.O. Nielsen, J-E.S. Hansen, J. Immunol. Methods 200 (1997) 107.
[23] L.A. Stanciu, J. Shute, S.T. Holgate, R. Djukanovi, J. Immunol. Methods 189 (1996) 107.
[24] S.T. Kim, D.-J. Kim, T.-J. Kim, D.-W. Seo, T.-H. Kim, S.-Y. Lee, K. Kim, K.-M. Lee, S.-K. Lee, Nano Lett. 10 (2010) 2877.
[25] H.L. Liu, C.H. Sonn, J.H. Wu, K.-M. Lee, Y.K. Kim, Biomaterials 29 (2008) 4003.

[26] K. Srithanaviboonchai, K. Rungruengthanakit, P. Nouanthong, S. Pata, T. Sirisanthana, W. Kasinrerk, J. Acquir. Immune Defic. Syndr. 47 (2008) 135.
[27] P. Nouanthong, S. Pata, T. Sirisanthana, W. Kasinrerk, Clin. Vaccine Immunol. (Clin. Diag. Lab. Immunol.) 13 (2006) 598.
[28] S. Chaleawlert-umpon, V. Mayen, K. Manotham, N. Pimpha, J. Biomater. Sci. 21 (2010) 1515.
[29] S. Ayyappan, G. Gnanaprakash, G. Panneerselvam, M.P. Antony, J. Philip, J. Phys. Chem. C 112 (2008) 18376.
[30] W.R. Viali, G.B. Alcantara, P.P.C. Sartoratto, M.A.G. Soler, E. Mosiniewicz-Szablewska, B. Andrzejewski, P.C. Morais, J. Phys. Chem. C 114 (2010) 179.
[31] J.M. Jin, J.M. Lee, M.H. Ha, K. Lee, S. Choe, Polymer 48 (2007) 3107.
[32] S. Chairam, E. Somsook, J. Magn. Magn. Mater. 320 (2008) 2039.
[33] M. Chen, Y.N. Kim, C. Li, S.O. Cho, J. Phys. Chem. C 112 (2008) 6710.
[34] M. Mikhaylova, D.K. Kim, N. Bobrysheva, M. Osmolowsky, V. Semenov, T. Tsakalakos, M. Muhammed, Langmuir 20 (2004) 2472.
[35] M. Chastellain, A. Petri, H. Hofmann, J. Colloid Interface Sci. 278 (2004) 353.
[36] K.E. McCloskey, J.J. Chalmers, M. Zborowski, Anal. Chem. 75 (2003) 6868.
[37] B. Xue, Y. Sun, J. Chromatogr. A 947 (2002) 185.